

## Antiaromaticity in Fluorenylidene Dications. Experimental and Theoretical Evidence for the Relationship between the HOMO/LUMO Gap and Antiaromaticity

Nancy S. Mills,\* Amalia Levy, and Benjamin F. Plummer<sup>1</sup>

Department of Chemistry, Trinity University, San Antonio, Texas 78212-7200

*nmills@trinity.edu*

Received January 12, 2004

The relationship between the calculated energy of the HOMO–LUMO gap, where  $(\epsilon_{\text{LUMO}} - \epsilon_{\text{HOMO}})/2$  is defined as  $\Delta_{\text{HL}}$ , and of the longest wavelength transition in the UV–visible spectrum,  $\Delta E$ , was examined for a series of aromatic and antiaromatic cations and dications. TD-DFT calculations accurately modeled the energies of a series of dications including fluorenylidene dications whose UV–visible spectra are reported, as well as the energies of a series of aromatic and antiaromatic monocations whose spectra were previously reported. There is a linear correlation of the energy of the longest wavelength transition,  $\Delta E_{\text{calc}}$ , with  $\Delta_{\text{HL}}$ . There is no linear relationship between  $\Delta E_{\text{calc}}$  and the sum of the NICS values, but there is a linear relationship between  $\Delta E_{\text{calc}}$  multiplied by the number of atoms in the conjugated system,  $\Delta E_{\text{calc(T)}}$ , and the sum of the NICS values. There is also an approximate linear relationship between the average <sup>1</sup>H NMR shift and the sum of the NICS values. These relationships give further support to the suggestion that the magnetic and energetic criteria of aromaticity and antiaromaticity are related. Furthermore, the data suggest that species that have  $\Delta E_{\text{calc(T)}} < 20$  are antiaromatic whereas those with  $\Delta E_{\text{calc(T)}} > 30$  are aromatic.

Although the concept of aromaticity and, by extension, antiaromaticity has general acceptance among the chemical community, the nature of the experimental evidence used to validate the aromaticity of a compound or species has experienced a great deal of controversy.<sup>2–4</sup> In general, the criteria used to characterize aromaticity fall into three categories that are derived from properties of benzene: magnetic, structural, and energetic.<sup>5,6</sup> Briefly, magnetic criteria focus on the consequences of the existence of a ring current, which include magnetic susceptibility exaltation ( $\Lambda$ ),<sup>7</sup> nucleus independent chemical shift (NICS),<sup>8</sup> and diatropic shift of protons on the periphery of an aromatic ring system.<sup>9,10</sup> Interestingly, although the diatropic shift is probably the single most used measure of aromaticity, Schleyer has recently provided evidence that the downfield shift of protons on benzene is not due to the deshielding effects of the ring current.<sup>11</sup> An antiaromatic system would show values of

NICS,  $\Lambda$ , and potentially chemical shift that are opposite in sign to those of an aromatic system.<sup>12</sup> Structural criteria include lack of bond length alternation and can be evaluated through the harmonic oscillator model of aromaticity (HOMA).<sup>13–15</sup> Energetic criteria are based on the greater stability of an aromatic system over a comparable system with localized bonds. Antiaromatic systems would show a greater thermodynamic instability compared to that of an appropriate reference system.

If the evaluation of aromaticity is challenging, the evaluation of the antiaromaticity of a system is even more so, in part because of the lack of appropriate systems for examination. We have discovered a class of fluorenylidene dications that appear to be antiaromatic, on the basis of the criteria described above.<sup>16–23</sup> By examining

(1) Professor Emeritus, Trinity University.  
 (2) Schleyer, P. v. R.; Freeman, P. K.; Jiao, H.; Goldfuss, B. *Angew. Chem., Int. Ed. Engl.* **1995**, *16*, 337–340.  
 (3) Cyranski, M. K.; Krygowski, T. M.; Katritzky, A. R.; Schleyer, P. v. R. *J. Org. Chem.* **2002**, *67*, 1333–1338.  
 (4) Katritzky, A. R.; Karelson, M.; Sild, S.; Krygowski, T. M.; Jug, K. *J. Org. Chem.* **1998**, *63*, 5228–5231.  
 (5) Minkin, V. I.; Glukhovtsev, M. N.; Simkin, B. Y. *Aromaticity and Antiaromaticity*; John Wiley and Sons: New York, 1994.  
 (6) Glukhovtsev, M. J. *Chem. Educ.* **1997**, *74*, 132–136.  
 (7) Schleyer, P. v. R.; Jiao, H. *Pure Appl. Chem.* **1996**, *68*, 209–218.  
 (8) Schleyer, P. v. R.; Maerker, C.; Dransfeld, A.; Jiao, H.; Hommes, N. J. v. E. *J. Am. Chem. Soc.* **1996**, *118*, 6317–6318.  
 (9) Elvidge, J. A.; Jackman, L. M. *J. Chem. Soc.* **1961**, 859–866.  
 (10) Mitchell, R. H. *Chem. Rev.* **2001**, *101*, 1301–1316.  
 (11) Wannere, C. S.; Schleyer, P. v. R. *Org. Lett.* **2003**, *5*, 605–608.

(12) Krygowski, T. M.; Cyranski, M. K.; Hafelinger, G.; Katritzky, A. R. *Tetrahedron* **2000**, *56*, 1783–1796.  
 (13) Krygowski, T. M.; Cyranski, M. K. *Chem. Rev.* **2001**, *101*, 1385–1419.  
 (14) Kruszewski, J.; Krygowski, T. M. *Tetrahedron Lett.* **1972**, 3839–3842.  
 (15) Krygowski, T. M. *J. Chem. Inf. Comput. Sci.* **1993**, *33*, 70–78.  
 (16) Malandra, J. L.; Mills, N. S.; Kadlecik, D. E.; Lowery, J. A. *J. Am. Chem. Soc.* **1994**, *116*, 11622–11624.  
 (17) Mills, N. S.; Malandra, J. L.; Burns, E. E.; Green, A.; Unruh, K. E.; Kadlecik, D. E.; Lowery, J. A. *J. Org. Chem.* **1997**, *62*, 9318–9322.  
 (18) Mills, N. S.; Burns, E. E.; Hodges, J.; Gibbs, J.; Esparza, E.; Malandra, J. L.; Koch, J. *J. Org. Chem.* **1998**, *63*, 3017–3022.  
 (19) Mills, N. S.; Malinky, T.; Malandra, J. L.; Burns, E. E.; Crossno, P. *J. Org. Chem.* **1999**, *64*, 511–517.  
 (20) Mills, N. S. *J. Am. Chem. Soc.* **1999**, *121*, 11690–11696.  
 (21) Mills, N. S.; Benish, M. M.; Ybarra, C. *J. Org. Chem.* **2002**, *67*, 2003–2012.  
 (22) Mills, N. S. *J. Org. Chem.* **2002**, *67*, 7029–7036.  
 (23) Levy, A.; Rakowitz, A.; Mills, N. S. *J. Org. Chem.* **2003**, *68*.

the antiaromaticity of these systems, we hope to refine the way in which those criteria are used to define aromaticity. Those criteria are based upon properties of benzene; however, all properties of benzene are not necessarily related to the aromaticity of benzene. By examining the criteria in systems that are very far removed from benzene, we hope to highlight any weaknesses in the relationships of the criteria to aromaticity.

One problem with the assessment of aromaticity/antiaromaticity is that many of the criteria involve calculated rather than measured quantities. Although there is growing acceptance of the results of calculations, many chemists are more comfortable when those results are supported by experimental data. A particular problem exists in the assessment of the stability of a molecule or species because the choice of a reference system can be contentious. We were interested in exploring the use of the energy of the longest wavelength transition, which we will call  $\Delta E_{\text{exp}}$ , in the UV-visible spectrum as a measure of stability and therefore aromaticity.

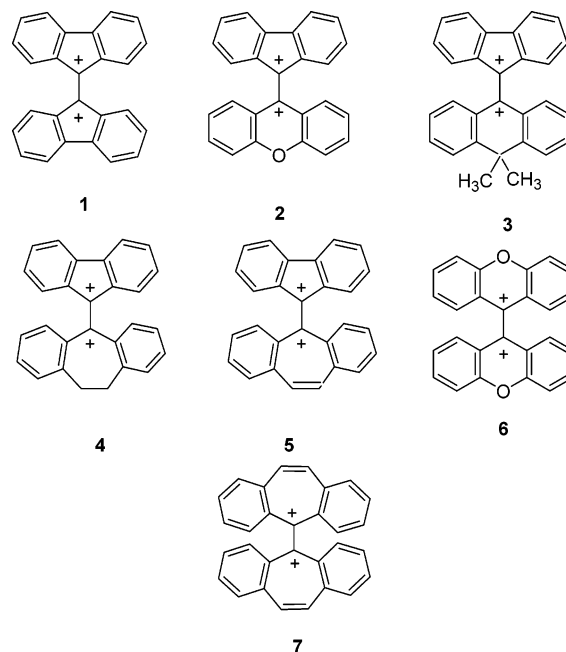
$\Delta E_{\text{exp}}$  has been shown to be related to the calculated HOMO-LUMO gap,  $(\epsilon_{\text{LUMO}} - \epsilon_{\text{HOMO}})$ .<sup>24–27</sup> Molecules with large HOMO-LUMO gaps have been shown to be stable and unreactive; those with small gaps are chemically reactive.<sup>28–32</sup> The theoretical basis for the relationship between the HOMO-LUMO gap and stability was articulated by Pearson and defined as hardness,  $\eta$ .<sup>33–35</sup> Operationally, hardness is related to the difference between the ionization energy ( $I$ ) and the electron affinity ( $A$ ) and, via Koopman's theorem, to the difference between the energy of the HOMO and that of the LUMO:<sup>33</sup>

$$\eta = \frac{I - A}{2} = \frac{\epsilon_{\text{LUMO}} - \epsilon_{\text{HOMO}}}{2} = \Delta_{\text{HL}}$$

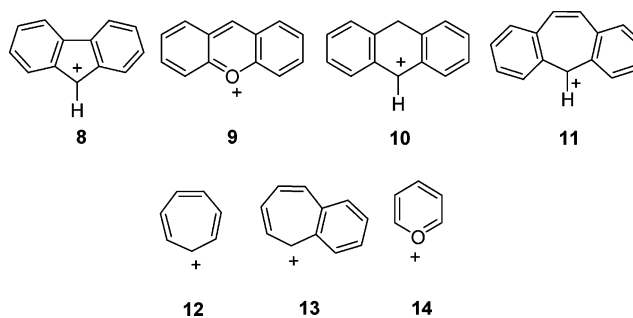
Because stability is one of the criteria used to assess aromaticity, hardness has been associated with aromaticity.<sup>36–38</sup> Global hardness, evaluated as  $\Delta_{\text{HL}}$  and calculated by density functional theory, has been shown to be a good measure of aromaticity/antiaromaticity for a series of five-membered heterocycles,  $C_4H_4X$ , through its strong correlation with magnetic susceptibility exaltation,  $\Lambda$ .<sup>39</sup> Other studies show a good correlation between hardness and measures of aromaticity such as REPE, resonance energy per electron.<sup>37</sup>

We were intrigued with the possibility of exploiting the relationship of hardness, a calculated measure of aro-

maticity/antiaromaticity, to an experimental observable,  $\Delta E_{\text{exp}}$ . Because hardness, and therefore  $\Delta_{\text{HL}}$ , is a measure of stability,  $\Delta E_{\text{exp}}$  could offer an experimental evaluation of stability that did not depend on the choice of a reference system. Our plan was first to confirm the relationship between  $\Delta_{\text{HL}}$  and  $\Delta E_{\text{exp}}$  and then to examine the relationship between  $\Delta E_{\text{exp}}$  and other measures of aromaticity, such as  $^1\text{H}$  NMR shift and NICS. We report here the experimental spectra for a series of fluorenylidene dications, **1–5**, as well as for the dications of 9,9'-dixanthyliene **6** and tetrabenzo[7.7]fulvalene **7**.



Calculation of the electronic spectra using TD-DFT methods revealed that  $\Delta E_{\text{exp}}$  for dications **1–5** would occur at very long wavelengths ( $>950$  nm) (see Table S1, Supporting Information) that were inaccessible to us because of experimental limitations. We therefore approached the problem by comparing the calculated spectra to the experimental spectra, in regions accessible to us. We attempted to improve the validity of this method of comparison by extending it to seven additional aromatic and antiaromatic cations, **8–14**, whose electronic



spectra were reported in the literature. Although our intent was to examine the relationship of  $\Delta E_{\text{exp}}$  to measures of aromaticity/antiaromaticity, our inability to observe  $\Delta E_{\text{exp}}$  for **1–5** required us to rely on the calculated values of the energy of the longest wavelength transition,  $\Delta E_{\text{calc}}$ . Thus, our initial goal of evaluating an

(24) Tagmatarchis, N.; Aslanis, E.; Prassides, K.; Shinohara, H. *Chem. Mater.* **2001**, *13*, 2374–2379.

(25) Makela, N. I.; Knuuttila, H. R.; Linnolahti, M.; Pakkanen, T. A. *Dalton Trans.* **2001**, 91–96.

(26) Belletete, M.; Beaupre, S.; Bouchard, J.; Blondin, P.; Leclerc, M.; Durocher, G. *J. Phys. Chem. B* **2000**, *104*, 9118–9125.

(27) Mitsui, M.; Ohshima, Y. *J. Phys. Chem. A* **2000**, *104*, 8638–8648.

(28) Zhou, Z.; Parr, R. G. *J. Am. Chem. Soc.* **1990**, *112*, 5720–5724.

(29) Gilman, J. J. *Mat. Res. Innovations* **1997**, *1*, 71–76.

(30) Aihara, J. *J. Phys. Chem. A* **1999**, *103*, 7487–7495.

(31) Aihara, J. *Phys. Chem. Chem. Phys.* **1999**, *1*, 3193–3197.

(32) Aihara, J. *Theor. Chem. Acta* **1999**, *102*, 134–138.

(33) Pearson, R. G. *J. Org. Chem.* **1989**, *54*, 1423–1430.

(34) Pearson, R. G. *Acc. Chem. Res.* **1993**, *26*, 250–255.

(35) De Proft, F.; Geerlings, P. *Chem. Rev.* **2001**, *101*, 1451–1464.

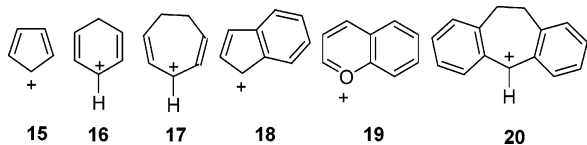
(36) Zhou, Z. *Int. Rev. Phys. Chem.* **1992**, *11*, 243–261.

(37) Zhou, Z.; Parr, R. G. *J. Am. Chem. Soc.* **1989**, *111*, 7371–7379.

(38) Zhou, Z.; Pearson, R. G. *Tetrahedron Lett.* **1988**, *29*, 4843–4846.

(39) Balawender, R.; Komorowski, L.; De Proft, F.; Geerlings, P. *J. Phys. Chem. A* **1998**, *102*, 9912–9917.

experimental observable,  $\Delta E_{\text{exp}}$ , was not possible, although we will argue that comparison of calculated and experimental UV–visible spectra support the use of  $\Delta E_{\text{calc}}$  in place of  $\Delta E_{\text{exp}}$ . Because the calculated values were good predictors of experimental electronic spectra, we were ultimately able to extend our studies to include dications **15–20**, for which electronic spectra had not been reported in the literature.



To summarize, this paper reports the electronic spectra for a set of seven dications. Those data, along with literature values for seven additional monocations, were used to evaluate the quality of TD-DFT calculations of the electronic spectra of these 14 mono- and dications.  $\Delta E_{\text{calc}}$  from the TD-DFT calculations were compared to  $\Delta H_{\text{L}}$  for **1–20** and exhibited a linear relationship.  $\Delta E_{\text{calc}}$  and an adjusted value of  $\Delta E_{\text{calc}}$ , *vide infra*, were then compared to the  $^1\text{H}$  NMR shift for dications **1–14** and to the NICS values for **1–20**.

## Results and Discussion

**UV–Visible Spectra of 1–7.** Dications **1–7** were prepared by oxidation of the neutral precursors in  $\text{SbF}_5$  in  $\text{SO}_2\text{ClF}$  or in  $\text{SO}_2\text{Cl}_2$  at temperatures varying from  $-30$  to  $0$  °C. Oxidation with  $\text{SbF}_5/\text{SO}_2\text{ClF}$  at  $-50$  °C was originally examined because these conditions were those in which dications **1–5** were originally characterized by NMR spectroscopy.<sup>17</sup> However, oxidation with  $\text{SbF}_5/\text{SO}_2\text{Cl}_2$  at  $-30$  to  $0$  °C gave identical spectra, so data for oxidations in  $\text{SO}_2\text{Cl}_2$  at  $-30$  °C are the ones reported here. The strongest absorptions for the UV–visible spectra of **1–7** and the absorptions for the corresponding monocations **8–14** for which UV–visible spectra are reported<sup>40–46</sup> are given in Table S2 in Supporting Information, along with the transitions calculated by TD-DFT spectra, using the 6-31G(d,p) basis set. TD-DFT calculations at the B3LYP/6-31G(d,p) level have been shown to give reasonable agreement with experimental spectra, with accuracies of 0.3 eV.<sup>47</sup> TD-DFT calculations of excited states are often remarkably improved relative to CIS with either gradient corrected or local density functionals.<sup>48</sup> The correlation between experimental and calculated spectra is shown in Figure 1.

The comparison of experimental with calculated spectra utilized the calculated transitions with the largest

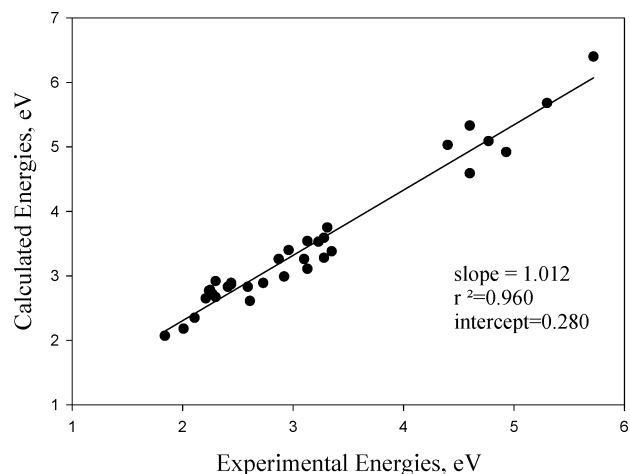


**FIGURE 1.** Calculated vs experimental energies of the electronic spectra for **1–14**.

oscillator strength.<sup>49</sup> However, the oscillator strengths associated with the longest wavelength transitions tended to be small, consistent with absorbances with small molar absorptivity, as is shown in Table S1 in Supporting Information. For dications **1–5**, those transitions were calculated to be in the long wavelength region inaccessible to us because of instrumental limitations, as previously mentioned. The literature data for **8–14** did not show absorbances at the wavelengths predicted by calculation, which also were calculated to have small oscillator strengths. These results could call into question the reliability of  $\Delta E_{\text{calc}}$ . We carefully examined the spectra of dications **6** and **7**, for which  $\Delta E_{\text{exp}}$  should be accessible. There was no evidence of absorbances with small molar absorptivities that would suggest that the calculated energy of the longest wavelength transition was very different from the experimental value.

The experimental support for the calculations justifies expansion of the study to include cations for which no experimental data exist. Thus, Table S1 also includes the calculated values for the monocations **15–20**.

**Correlation of the Energy of the Longest Wavelength Transition with the HOMO–LUMO Gap.** The calculated energy of the longest wavelength transition was first compared with the calculated  $\Delta H_{\text{L}}$ , which has been associated with aromaticity/antiaromaticity. The energies of the HOMO and LUMO and  $\Delta H_{\text{L}}$ , which is  $(\epsilon_{\text{LUMO}} - \epsilon_{\text{HOMO}})/2$  for **1–20**, are given in Table S3, Supporting Information. Because  $\Delta H_{\text{L}}$  is suggested to be small for antiaromatic species, it is possible that the triplet energy for such a species might be lower in energy than the singlet. Calculations of **15** show that the triplet state is lower than the singlet.<sup>50,51</sup> However, calculations for **1–5**, the fluorenyl cation **8**, and the indenyl cation **18** show the singlet state to be lower in energy than the

(40) McClelland, R. A. M.; Steenken, S. *J. Am. Chem. Soc.* **1990**, *112*, 4857–4861.

(41) Cozens, F. L.; Cano, M. L.; Garcia, H.; Schepp, N. P. *J. Am. Chem. Soc.* **1998**, *120*, 5667–5673.

(42) Morita, M.; Hirosawa, K.; Sato, T.; Ouchi, K. *Bull. Chem. Soc. Jpn.* **1981**, *54*, 540–544.

(43) Naville, G.; Strauss, H.; Heilbronner, E. *Helv. Chim. Acta* **1960**, *43*, 1221–1243.

(44) Stanescu, M. D. *Roum. Chem. Quart. Rev.* **1996**, *4*, 107–121.

(45) Meier, W.; Meuche, D.; Heilbronner, E. *Helv. Chim. Acta* **1962**, *45*, 2628–2650.

(46) Yoshida, Z.; Sugimoto, H.; Yoneda, S. *Tetrahedron* **1972**, *28*, 5873–5881.

(47) Szczepanski, J.; Banisaukas, J.; Vala, M.; Hirata, S.; Bartlett, R. J.; Head-Gordon, M. *J. Phys. Chem. A* **2002**, *106*, 63–73.

(48) Kong, J.; White, C. A.; Krylov, A. I.; Sherrill, D.; Adamson, R. D.; Furlani, T. R.; Lee, M. S.; Lee, A. M.; Swaltney, S. R.; Adams, T. R.; Ochsenfeld, C.; Gilbert, A. T. B.; Kedziora, G. S.; Rassovov, V. A.; Maurice, D. R.; Nair, N.; Shao, Y.; Besley, N. A.; Maslen, P. E.; Dombroski, J. P.; Daschel, H.; Zhang, W.; Korambath, P. P.; Baker, J.; Byrd, E. F. C.; Van Voorhis, T.; Oumi, M.; Hirata, S.; Hsu, C.-P.; Ishikawa, N.; Florian, J.; Warshel, A.; Johnson, B. G.; Gill, P. M. W.; Head-Gordon, M.; Pople, J. A. *J. Comput. Chem.* **2000**, *21*, 1532–1548.

(49) Baumann, H.; Martin, R. E.; Diederich, F. *J. Comput. Chem.* **1999**, *20*, 396–411.



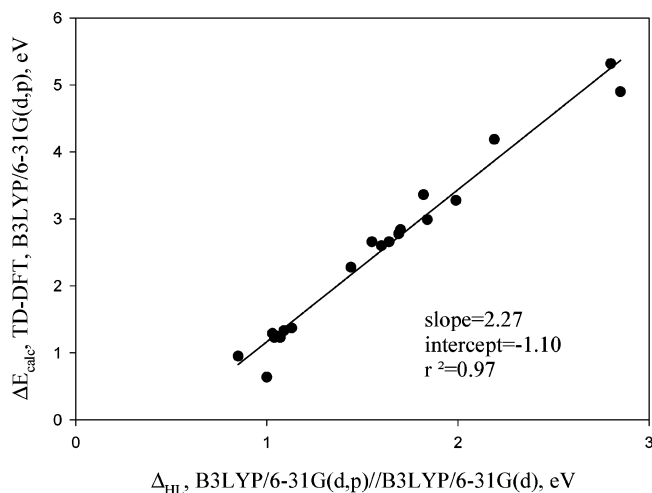


**FIGURE 2.** Plot of HOMO–LUMO energies vs energy of longest wavelength transition.

triplet state.<sup>22,51</sup> Thus, all mono- and dications except **15** are predicted to be singlets. Although the triplet state of **15** was calculated to be lower in energy than the singlet, calculations for **15** are reported only for the singlet state to maintain consistency with calculations for the other species.

Figure 2 shows the correlation between  $\Delta_{HL}$  at the B3LYP/6-31G(d,p) level and the energies of the longest wavelength transition,  $\Delta E_{calc}$ , calculated using the TD-DFT method at the same level for the geometries optimized at the B3LYP/6-31G(d) level. The relationship between these properties and aromaticity/antiaromaticity has been with hardness,  $\eta$ , which is equated to  $\Delta_{HL}$ , not with  $\Delta E_{calc}$  or  $\Delta E_{exp}$ , so it is appropriate to examine the assumptions made in relating  $\Delta E$  to  $\Delta_{HL}$ . The approach was used by Mitsui et al.,<sup>27</sup> and we reiterate their arguments. The method is based on the rough approximation that treats the  $S_1 \leftarrow S_0$  transition as an one-electron excitation from the HOMO to the LUMO. The molecular orbitals are assumed to be unchanged regardless of the electronic excitations. In Hartree–Fock theory, the energy of the HOMO, a measure of ionization potential using Koopman’s theorem, is considered reliable.<sup>52</sup> However, the energy calculated for the LUMO of the neutral molecule reflects the electron affinity of the anion rather than the electron affinity of the neutral molecule, which is necessary for accurate calculation of the energy of the HOMO–LUMO gap.<sup>53</sup> Thus, at the Hartree–Fock level, correlation of the energy of the HOMO–LUMO gap with excitation energies has not been reliable. It is not immediately apparent that this approach can be used with density functional theory calculations because the energies of these orbitals have no obvious physical meaning.<sup>54</sup> However, studies examin-

ing the relationship of experimental excitation energies to HOMO–LUMO gaps calculated by the TD-DFT method show that there is good agreement.<sup>25,27,54,55</sup> Our results also support this relationship. It now remains to explore the relationship between  $\Delta E_{calc}$  and other measures of aromaticity/antiaromaticity.

**Correlation with UV–Visible Spectra and Measures of Aromaticity/Antiaromaticity.** The HOMO–LUMO gap,  $\Delta_{HL}$ , is related to the concept of hardness that is a reflection of stability/reactivity. Thus the HOMO–LUMO gap reflects the *energetic* criterion of aromaticity. Stability has also been assessed by comparison with appropriate reference systems, to give the aromatic stabilization energies.<sup>56,57</sup>

It is of interest to examine the relationship of the energy of the longest wavelength transition,  $\Delta E$ , to other criteria of aromaticity. We have previously suggested that the *structural* criterion of aromaticity that is reflected in the lack of bond length alternation is not particularly useful when examining polycyclic aromatic hydrocarbons whose bond length changes are limited by their benzannulation.<sup>22</sup>

Magnetic criteria, based on the special behavior associated with induced ring currents, have been suggested as the most important of the three criteria.<sup>3</sup> The nucleus independent chemical shift (NICS)<sup>8</sup> has been shown to be an effective measure of aromaticity/antiaromaticity, and NICS values have recently been correlated with experimental measures of aromaticity<sup>58</sup> and antiaromaticity.<sup>21–23</sup> NICS values are calculated at the center of the ring system of interest and are negative for aromatic ring systems and positive for antiaromatic systems. Because “local shielding effects” influence the magnitude of NICS, particularly for small rings, it has been recommended that they be calculated 1 Å above the plane of the ring.<sup>59</sup> The NICS values for **1–20** calculated 1 Å above the ring system are reported in Table S4 in Supporting Information, along with the sum of the NICS values. NICS values have been calculated using a variety of basis sets and show a dependence upon the basis set used.<sup>20</sup> We have calculated them at the B3LYP/6-31G(d) level because our calculations at that level on **1–5** and other fluorenylidene dications show that this basis set gives the best agreement of calculated NMR shift with experimental shift and presumably the most reliable value for NICS.<sup>20–23</sup> A number of recent papers also utilize NICS values calculated with this basis set.<sup>60–62</sup> Although NICS values evaluate local aromaticity, Schleyer has suggested that the summation of NICS values can be used to reflect global aromaticity(antiaromaticity).<sup>63</sup> For dications **1–5**, we also report the summation for the

(55) Wang, Z.; Day, P. N.; Pachter, R. J. *J. Chem. Phys.* **1998**, *108*, 2504–2510.

(56) Zhou, L.; Zhang, Y.; Wu, L.; Li, J. *THEOCHEM* **2000**, *497*, 137–144.

(57) Schleyer, P. v. R.; Puehlofer, F. *Org. Lett.* **2002**, *4*, 2873–2876.

(58) Williams, R. V.; Armantrout, J. R.; Twamley, B.; Mitchell, R. H.; Ward, T. R.; Bandyopadhyay, S. *J. Am. Chem. Soc.* **2002**, *124*, 13495–13505.

(59) Schleyer, P. v. R.; Manoharan, M.; Wang, Z.-X.; Kiran, B.; Jiao, H.; Puchta, R.; Hommes, N. J. R. v. E. *Org. Lett.* **2001**, *3*, 2465–2468.

(60) Okazaki, T.; Laali, K. K. *J. Org. Chem.* **2004**, *69*, 510–516.

(61) Moran, D.; Stahl, F.; Bettinger, H. F.; Schaefer, H. F., III; Schleyer, P. v. R. *J. Am. Chem. Soc.* **2003**, *125*, 6746–6752.

(62) Okazaki, T.; Laali, K. K. *Org. Biomol. Chem.* **2003**, *1*, 3078–3093.

(63) Schleyer, P. v. R.; Manoharan, M.; Jiao, H.; Stahl, F. *Org. Lett.* **2001**, *3*, 3643–3646.

(50) Gogonea, G.; Schleyer, P. v.; Schreiner, P. R. *Angew. Chem., Int. Ed.* **1998**, *37*, 1945–1948.

(51) Jiao, H.; Schleyer, P. v. R.; Mo, Y.; McAllister, M. A.; Tidwell, T. T. *J. Am. Chem. Soc.* **1997**, *119*, 7075–7083.

(52) Kimura, K.; Katsumata, S.; Achiba, Y.; Yamazaki, T.; Iwata, S. *Handbook of HeI Photoelectron Spectra of Fundamental Organic Molecules*; Halsted Press: New York, 1981.

(53) Hunt, W. J.; Goddard, W. A., III. *Chem. Phys. Lett.* **1969**, *3*, 414–418.

(54) Salzner, U.; Lagowski, J. B.; Pickup, P. G.; Poirier, R. A. *J. Comput. Chem.* **1997**, *18*, 1943–1953.

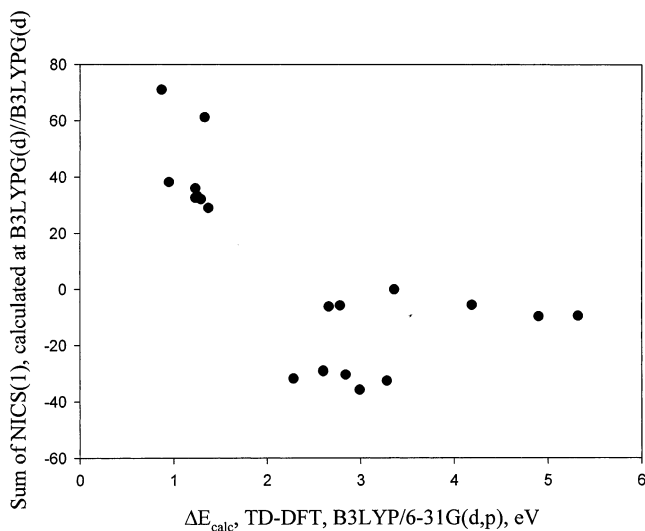


**FIGURE 3.**  $\Delta E_{\text{calc}}$  vs Sum of NICS(1) for **1–20**.

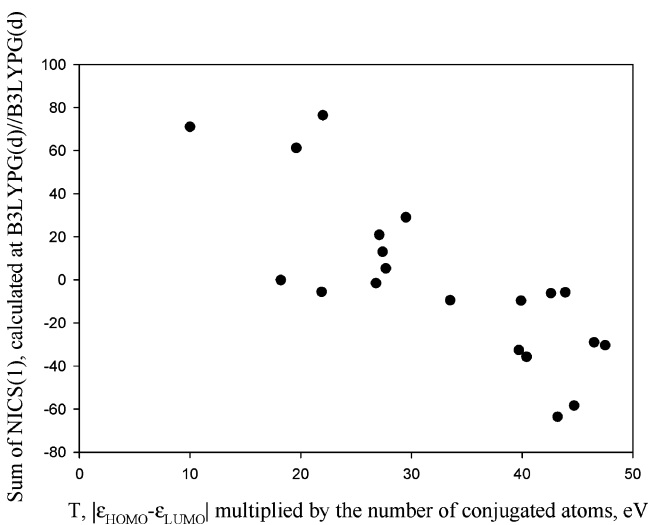


**FIGURE 4.**  $T$  vs sum of NICS(1), **1–20**.

fluorenyl rings only. The correlation of the sum of the NICS values with  $\Delta E_{\text{calc}}$  is shown in Figure 3 and is obviously not linear. As would be expected from the linear relationship of  $\Delta E_{\text{calc}}$  and  $\Delta_{\text{HL}}$ , the plot of the sum of the NICS(1) values vs  $\Delta_{\text{HL}}$  shows the same relationships as were true for the correlation of NICS(1) with  $\Delta E_{\text{calc}}$ .

Because the magnitude of  $\Delta_{\text{HL}}$  depends on the size of the conjugated system as well as on its potential aromaticity/antiaromaticity,<sup>35</sup> Aihara has suggested a new index, the  $T$  value in which the HOMO–LUMO gap is multiplied by the number of conjugated atoms.<sup>31,32,64</sup> The correlation of the sum of the NICS values with  $T$  is shown in Figure 4 and is more linear than the correlation with either  $\Delta E_{\text{calc}}$  or  $\Delta_{\text{HL}}$ . However, the graph shows a great deal of scatter.

Close analysis of the graph shows that the scatter is due primarily to two groups of compounds, those in which there is incomplete conjugation (**10**, **16**, **17**, and **20**) and to the dicationic systems, **1–7**. Previous studies on the

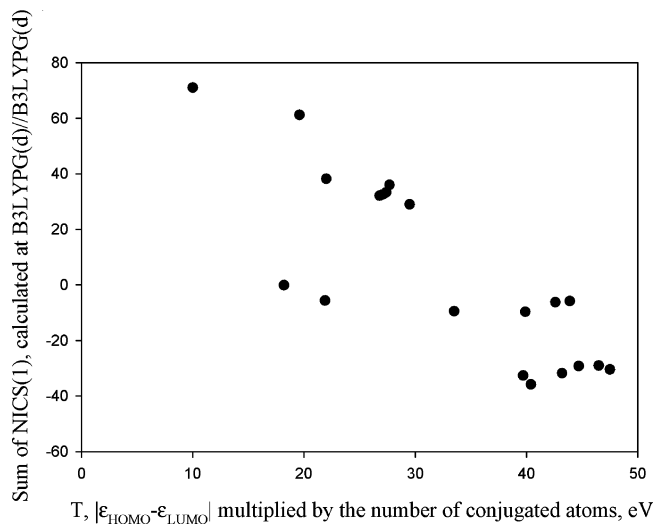


**FIGURE 5.**  $T$  vs sum of NICS(1), **1–20**. Only the NICS for the fluorenyl ring system of **1–5** are used.

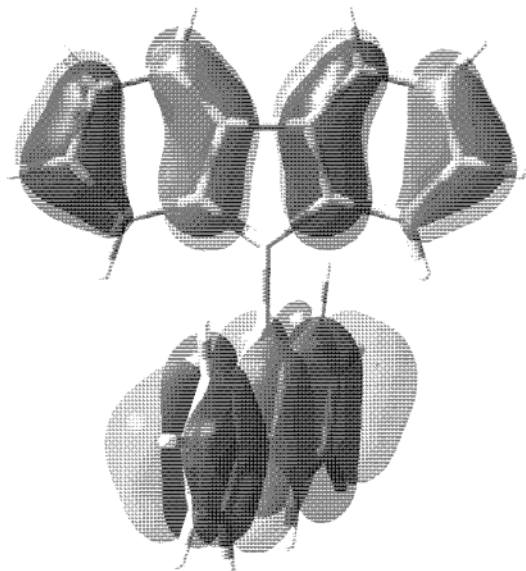
fluorenylidene dications showed that each existed as two perpendicular ring systems, with substantial antiaromaticity in the fluorenyl portion of the dication.<sup>17,22</sup> Analogously, the geometries calculated for **6** and **7** also reveal that the ring systems are perpendicular. Because  $\Delta E_{\text{calc}}$  for **1–5** was very small, a result that would be consistent with an antiaromatic system, we evaluated the relationship of  $T$  vs the summation of the NICS values considering only the fluorenyl systems of **1–5**. For consistency, we treated the ring systems of **6** and **7** analogously. This plot is shown in Figure 5. The two points that lie off the apparent line belong to **16** and **17**. When they and **10** and **20** are removed from the plot,  $r^2 = 0.92$  (see Supporting Information for this plot).

Some justification for this treatment lies in an examination of the HOMO and LUMO for **1–5**, which are shown in Figure 6. The TD-DFT calculations for **1–4** show that the calculation of the excited state with the lowest energy includes a substantial contribution for the promotion of an electron from the HOMO to the LUMO. That is, the largest coefficient in the CI expansion, which is greater than 0.66 for these systems, is for the contribution from that transition. Those molecular orbitals for **2–4** primarily involve the fluorenyl system. The lowest energy excited state for **1** of necessity involves a fluorenyl system because **1** only possesses fluorenyl systems. The HOMO for **5** involves the tropylium system; however, the lowest energy excited state involves the transition from the HOMO-1 to the LUMO, both of which primarily involve the fluorenyl system.

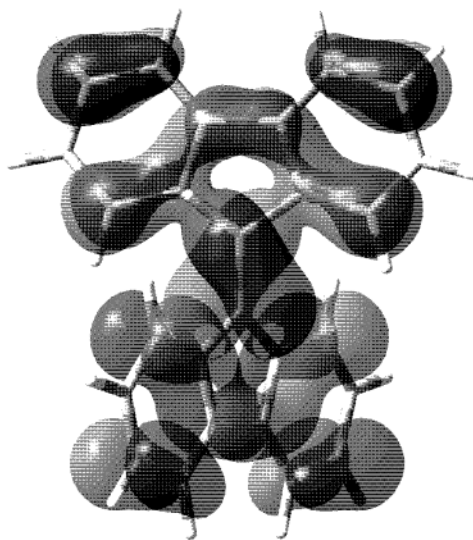
However,  $\Delta_{\text{HL}}$  is a calculated value, and we were interested in using an experimental value,  $\Delta E_{\text{exp}}$ , or the calculated value,  $\Delta E_{\text{calc}}$ , which could be related to an experimental value. We therefore examined the analogous treatment of  $\Delta E_{\text{calc}}$ , in which the values of  $\Delta E_{\text{calc}}$  were multiplied by the number of atoms in the conjugated system. Figure 7 shows the relationship between this modified value of  $\Delta E_{\text{calc}}$ , which we will call  $\Delta E_{\text{calc}}(T)$ , and the sum of the NICS(1) values, using only the fluorenyl ring system for **1–5**. Again the relationship is linear. When **10**, **16**, **17**, and **20** are removed,  $r^2 = 0.94$ ; see Supporting Information. Thus there is an excellent

(64) Yoshida, M.; Aihara, J. *Phys. Chem. Chem. Phys.* **1999**, *1*, 227–230.

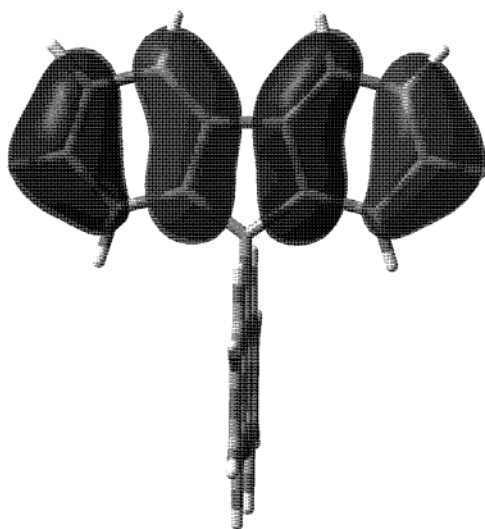
1, HOMO



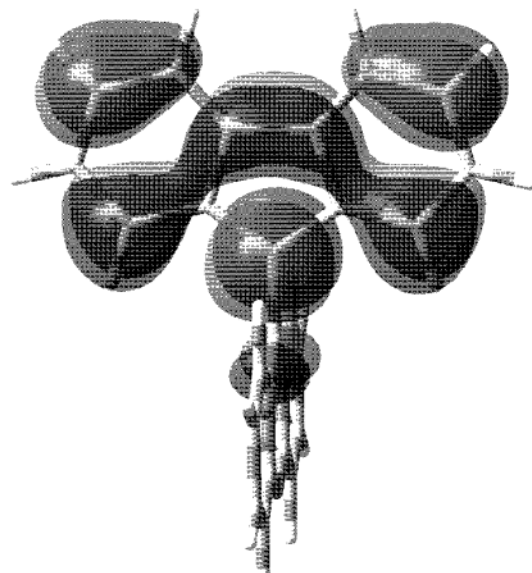
1, LUMO



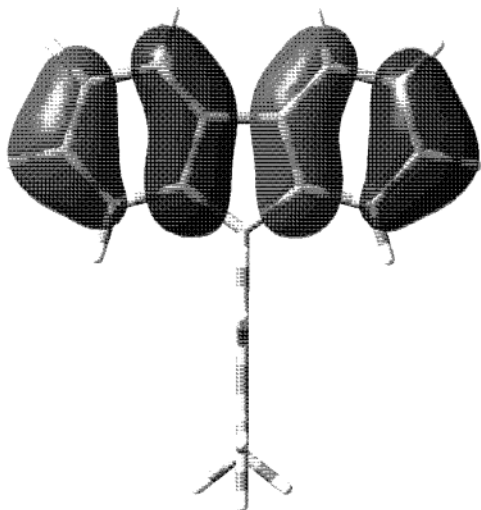
2, HOMO



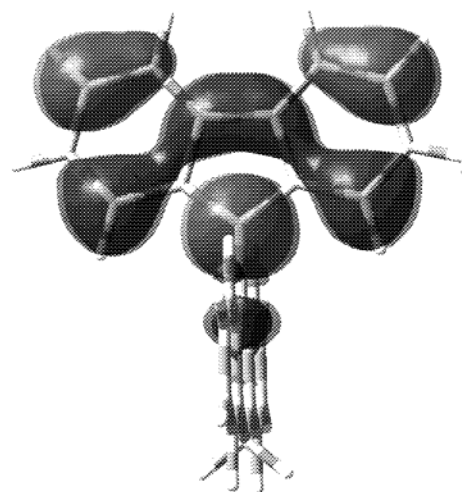
2, LUMO



3, HOMO

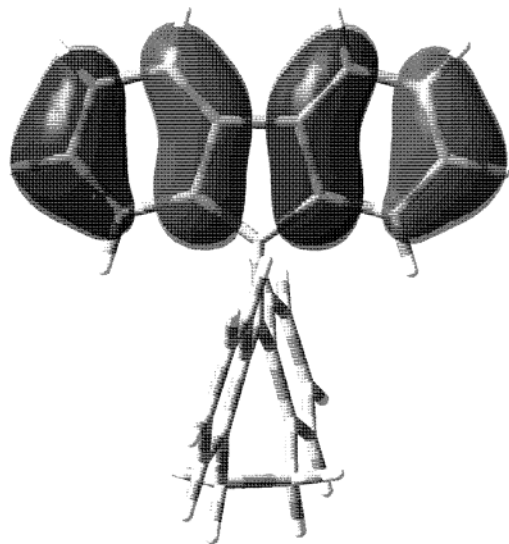


3, LUMO

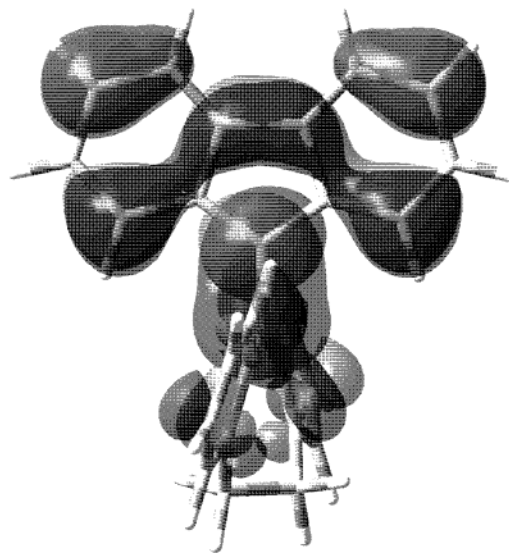




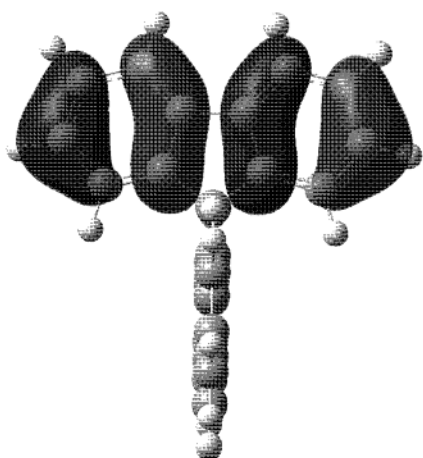
4, HOMO



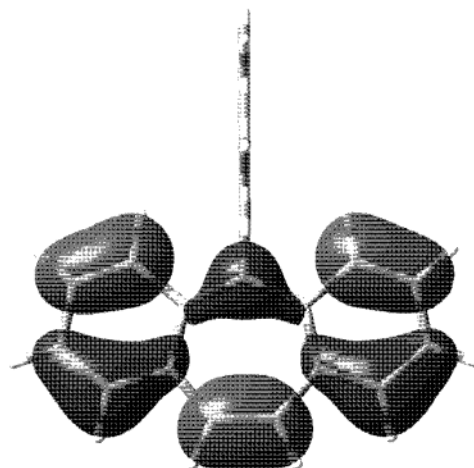
4, LUMO



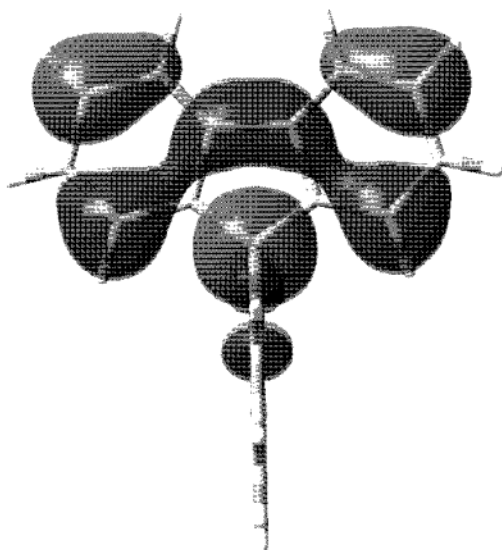
5, HOMO-1 (Molecular orbital 91)



5, HOMO (Molecular orbital 92)



5, LUMO (Molecular orbital 93)

**FIGURE 6.** Molecular orbitals calculated by TD-DFT, B3LYPO/6-31g(d,p).

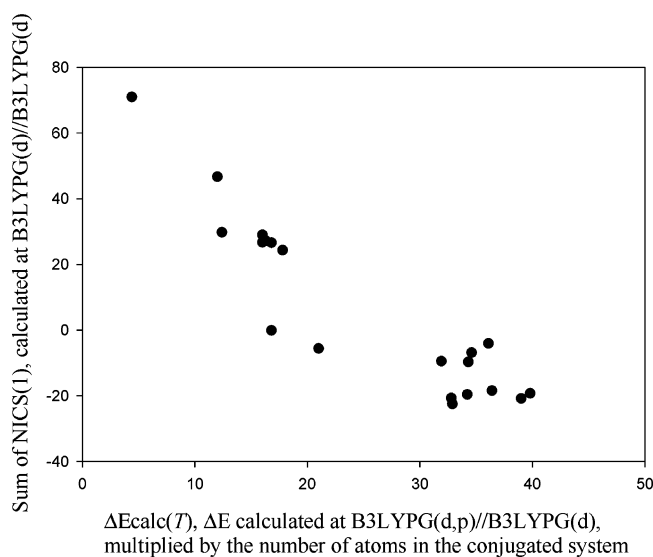


**FIGURE 7.** ( $\Delta E_{\text{calc}} \times \text{atoms}$ ) vs sum of NICS(1), **1–20**.

correlation between a measure of stability, reflecting the energetic criteria, and a measure of the ring current, reflecting the magnetic criteria. Of importance to the assessment of aromaticity and antiaromaticity, the cations and dications that remain after **16** and **17**, which possess no benzene rings, are excluded fall into two distinct groupings, a set of cations/dications suggested to be antiaromatic, with  $\Delta E_{\text{calc}(T)} < 20$  and those for which NICS values are negative and therefore aromatic, which have  $\Delta E_{\text{calc}(T)} > 30$ .

Although the relationship between the sum of the NICS(1) values and  $\Delta E$  was gratifying, we wanted to examine the relationship between an experimental measure of ring currents and this “experimental” measure of stability.  $^1\text{H}$  NMR shifts have been seen as the primary indicator of aromaticity/antiaromaticity, although the relationship between proton chemical shifts and ring currents has recently been called into question.<sup>11</sup> It is inappropriate to consider the average chemical shift for dications **1–5** because the protons on positions 1/8 and 2/7 of the fluorenyl system are affected by the opposing ring system.<sup>17</sup> For that reason, we have examined only the relationship between  $\Delta E_{\text{calc}}$  and the remaining species for which proton shifts are available in the literature, monocations **9**, **11–14**, and **20**.<sup>65–73</sup> The relationship between the average shift and  $\Delta E_{\text{calc}}$  multiplied by the number of atoms in the conjugated system is shown in Figure 8. The relationship is roughly linear, with data for **14** and **20** furthest from the apparent line. One might argue that **14**, because it is the only species with a

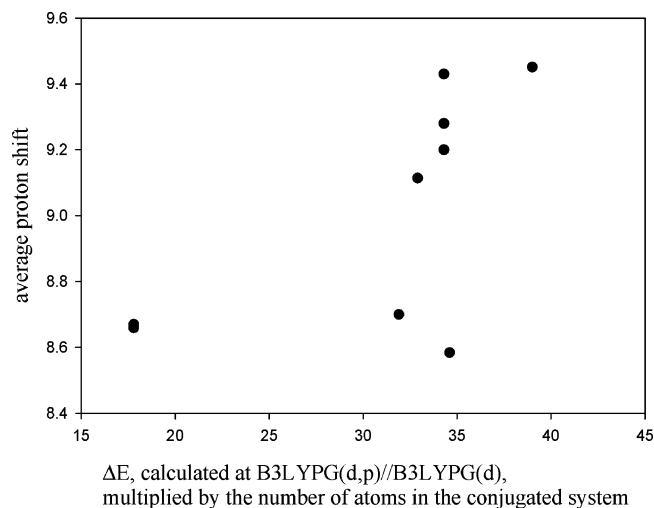


**FIGURE 8.** ( $\Delta E_{\text{calc}} \times \text{atoms}$ ) vs the average proton shift, **9**, **11–14**, **20**.

heteroatom, or **20**, the only species in which the conjugation is not complete, might not be expected to have the same linear relationship as the other species. Even with the remaining species, the spectra would be expected to show only an approximate linearity because they were taken in a variety of solvents, such as liquid  $\text{SO}_2$ , acetonitrile, concentrated sulfuric acid, and Magic Acid, respectively. In addition, the counterions varied from azide and thiocyanate to the conjugate base of the acid used to protonate the alcohol precursor. Both counterion and solvent would be expected to affect the magnitude of the chemical shift, as shown by the differences in chemical shift for the same ion; see Supporting Information. However, Figure 8 suggests the possibility that a linear relationship might be observed if all cations were prepared under the same conditions.

**Comparison between UV–Visible Spectra of Dications and Monocations.** Dications **1–5** have been shown to possess perpendicular ring systems, and calculations suggest that this is the case for **6** and **7** also. If so, it is of interest to see whether the UV–visible spectra for the dications are effectively composites of the spectra of the individual monocations. We show the comparison of composite spectra with the spectra of each dication in Figure 9. We have chosen to use the data calculated using the TD-DFT method rather than experimental data because this allows us to examine all seven dications. In addition, the data show the energies associated with the longest wavelength transitions that are anticipated to have small molar absorptivities because the calculated spectra have small oscillator strengths. The plots of the data show that **1–5** are not simply composites of the spectra of the individual monocations. The plots show that **1–5** are more antiaromatic than the fluorenyl monocations and that the energy of the longest wavelength transition is affected by the cationic substituent on position 9 in the fluorenylidene dications. That is, modification of the cyclic substituent at position 9 (in the box), see Figure 10, affects  $\Delta E_{\text{calc}}$ , from Tables S1 and S2, even though the ring systems are roughly perpendicular. We have seen similar effects on  $^1\text{H}$  NMR spectra, NICS, and magnetic susceptibility. The presence of the cationic substituent also acts to decrease DE for dications

(65) Kessler, H.; Walter, A. *Angew. Chem.* **1973**, *85*, 821–822.

(66) Feigel, M.; Kessler, H.; Leibfritz, D.; Walter, A. *J. Am. Chem. Soc.* **1979**, *101*, 1943–1950.

(67) Dradi, E.; Gatti, G. *J. Am. Chem. Soc.* **1975**, *97*, 5472–5476.

(68) Olah, G. A.; Liang, G. *J. Org. Chem.* **1975**, *40*, 2108–2116.

(69) Guenther, H.; Shyokh, A.; Cremer, D.; Frisch, K. H. *Justus Liebig's Ann. Chem.* **1978**, 150–164.

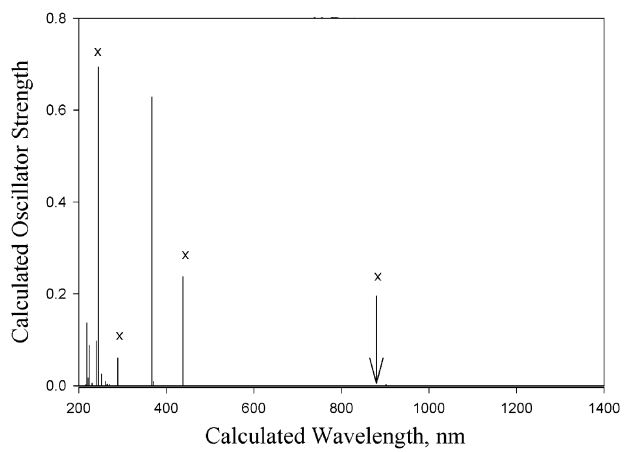
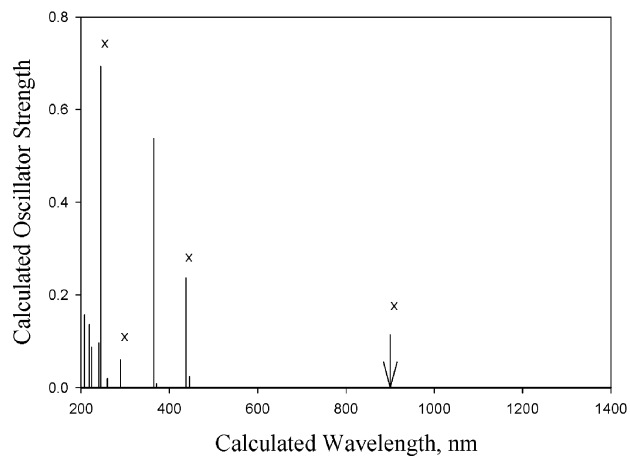
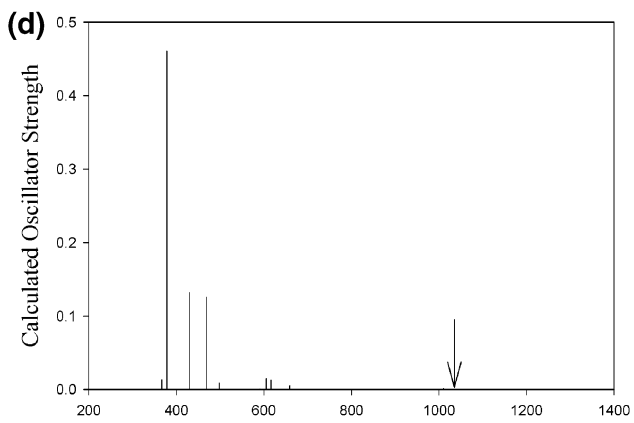
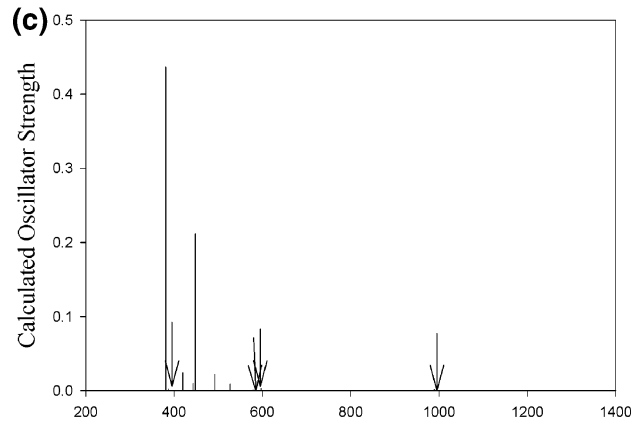
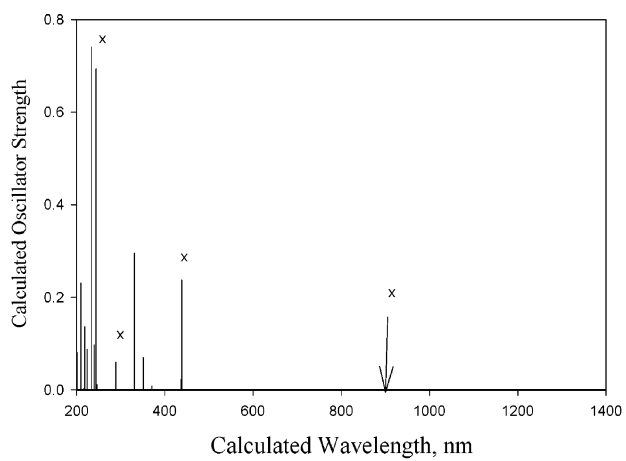
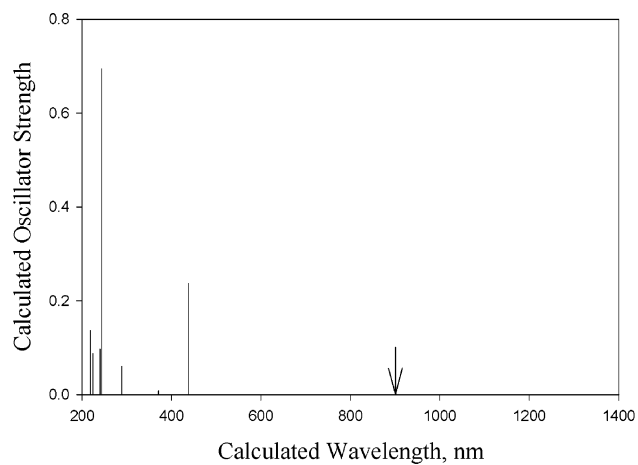
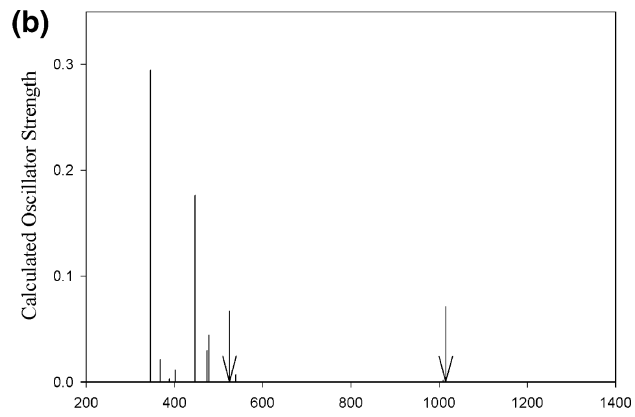
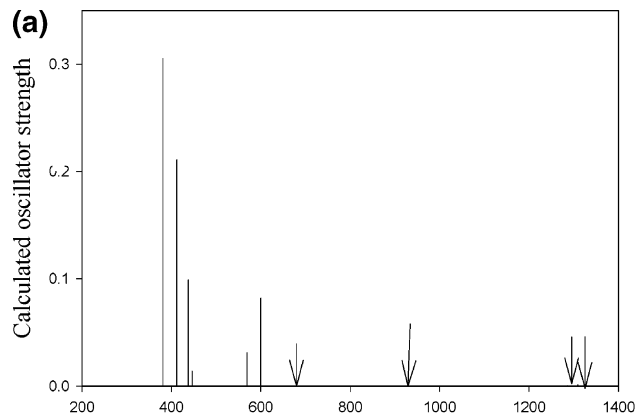
(70) Vilceanu, R.; Balint, A.; Simon, Z.; Rentia, C.; Unterweger, G. *Rev. Roum. Chim.* **1968**, *13*, 1623–1633.

(71) Radics, L.; Kardos, J. *Org. Magn. Reson.* **1973**, *5*, 251–252.

(72) Convert, O.; Le Roux, J. P.; Desbene, P. L.; Defoin, A. *Bull. Soc. Chim. Fr.* **1975**, 2023–2025.

(73) Rentia, C. C.; Balaban, A. T.; Simon, Z. *Rev. Roum. Chim.* **1966**, *11*, 1193–1203.





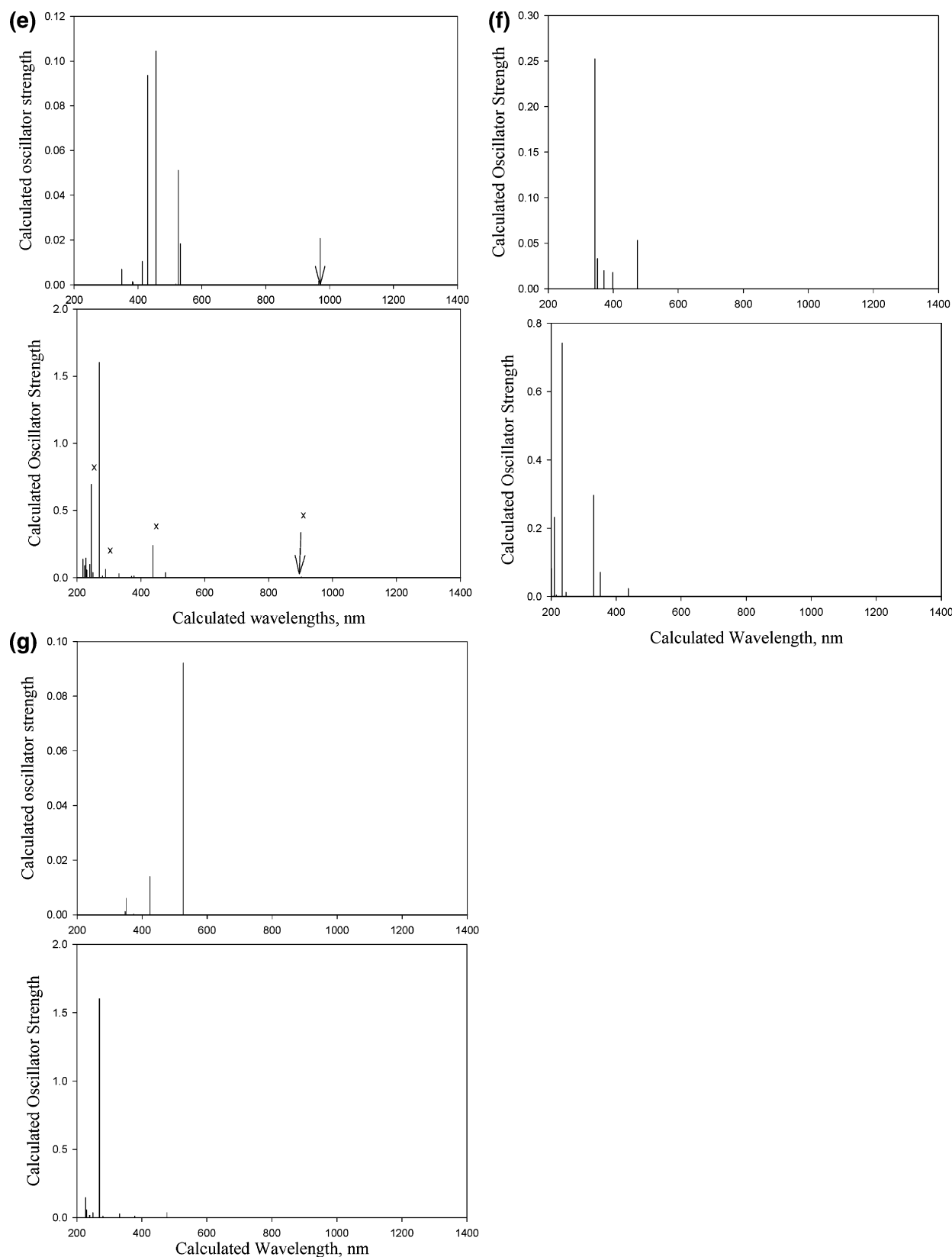


**FIGURE 9.** Comparison of calculated spectra for dications **1–7** with composite spectra for corresponding monocations **8–11** and **20**, respectively. Long wavelength transitions with very small oscillator strengths are indicated by arrows. (a) Comparison of **1** (top) with **9** (bottom). Arrows indicate absorptions with frequencies below 0.001. (b) Comparison of **2** (top) with composite of **8** and **9** (bottom). Peaks for **8** indicated by \* in long wavelength region. (c) Comparison of **3** (top) with composite of **8** and **10** (bottom). Peaks for **8** indicated by × in long wavelength region. (d) Comparison of **4** (top) with composite of **8** and **20** (bottom). Peaks for **8** indicated by × in long wavelength region. (e) Comparison of **5** (top) with composite of **8** and **11** (bottom). Peaks for **8** indicated by × in long wavelength region. (f) Comparison of **6** (top) with **9** (bottom). (g) Comparison of **7** (top) with **11** (bottom).

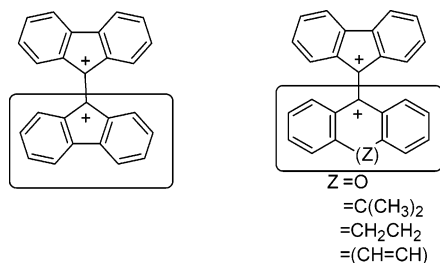
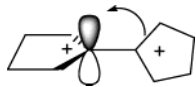


FIGURE 10.

**6** and **7** in comparison with their monocation analogues. The TD-DFT calculations show that the energy of the lowest excited state for **1–4** is primarily associated with the HOMO and LUMO, which are “fluorenyl-based” orbitals. Analogously, the orbitals of **5** that contribute to the lowest energy excited state are based on the fluorenyl system.

However, the observation that the spectra of **1–5** are not composites of the spectra of the individual ring systems comprising **1–5** suggests that there must be interaction between the two essentially orthogonal systems. We have suggested two explanations for the manner in which perpendicular ring systems can interact with each other. The magnitude of the charge on the opposing ring system can affect the degree to which the charge is delocalized throughout the ring system.<sup>22</sup> Alternatively,  $\sigma$  to  $p$  donation, also known as cross-hyperconjugation, as shown below for **1**, with the benzene rings eliminated for clarity, allows the ring systems to interact, even though they are perpendicular.<sup>16–18,21,22,74,75</sup>



**Summary.** TD-DFT calculations of the electronic spectra exhibit a strong linear correlation with experimental UV–visible spectra for aromatic and antiaromatic cations. There is a good linear relationship between the highest wavelength transition for these cations and  $\Delta_{HL}$ . There was no linear relationship between  $\Delta E_{calc}$  and the sum of the NICS values. There was a linear relationship between  $\Delta E_{calc}$  multiplied by the number of atoms in the conjugated system,  $\Delta E_{calc(T)}$ , and the sum of the NICS

values, when NICS values for the ring systems implicated in  $\Delta E_{calc}$  are used. The plot of the average  $^1\text{H}$  NMR shift vs the sum of the NICS values suggests a possible linear relationship. These results give further support to the suggestion that the magnetic and energetic criteria of aromaticity and antiaromaticity are related.<sup>2</sup> Furthermore, the data suggest that species that have  $\Delta E_{calc(T)} < 20$  are antiaromatic whereas those with  $\Delta E_{calc(T)} > 30$  are aromatic. If this relationship holds true for other systems, this would give another measure of aromaticity that is directly related to experimental data.

## Experimental Section

Compounds **1–7** were synthesized by literature methods.<sup>17,76,77</sup>

**Dication Preparation.**  $\text{SbF}_5$  (~7 mL, ~9 mmol) was added to a graduated centrifuge tube in a drybox, and the tube was capped with a septum. When  $\text{SO}_2\text{ClF}$  was used as the solvent, the  $\text{SbF}_5$  was cooled to 0 °C and  $\text{SO}_2\text{ClF}$  (1.2 mL, at –78 °C) was added by cannula. The reagents were mixed on a vortex-stirrer and rapidly cooled to –78 °C. When  $\text{SO}_2\text{Cl}_2$  was used as the solvent, the  $\text{SbF}_5$  was mixed with  $\text{SO}_2\text{Cl}_2$  (1.2 mL) at room temperature under argon and cooled to –30 °C. Approximately 1 mg of the dication precursor (2.6–3.0 mmol) was added under argon, and the solution was mixed on a vortex stirrer. Approximately 0.3 mL of this solution was transferred by cannula to 1.2 mL of pure solvent at –78 °C ( $\text{SO}_2\text{ClF}$ ) or –30 °C ( $\text{SO}_2\text{Cl}_2$ ). The solution was transferred to a gastight cell with a path length of 0.1 cm, and spectra were recorded from 300 to 900 nm. A reference solution without dication precursor was prepared similarly, and its spectrum was subtracted from that of the dication.

**Computational Details.** Geometries were optimized at B3LYP/6-31G(d) density functional theory levels with the Gaussian 98 and 03 program packages.<sup>78,79</sup> The energies of the 12 lowest excited states were calculated using the TD-DFT formalism, as implemented in Gaussian 98 and 03 and using the B3LYP/6-31G(d,p) functional on geometries optimized at the B3LYP/6-31G(d) level. The nucleus-independent chemical shifts (NICS<sup>8</sup>) in the ring centers were calculated at B3LYP/6-31G(d) using the GIAO approach with Gaussian 98 or 03.

**Acknowledgment.** We gratefully acknowledge the Welch Foundation (Grant 794) and the National Science Foundation (Grant CHE-0242227) for their support of this work.

**Supporting Information Available:** Absorption spectra for **1–7**; table of calculated symmetries, total energies, and  $[x,y,z]$  coordinates for **1–20**; table of all calculated wavelengths and energies for **1–20**; table of the literature values for the proton shifts of **9, 11–14, 20**; and plots of  $T$  and  $\Delta E_{calc}$  vs  $\Sigma\text{NICS}(1)$  for **1–9, 11–15, 18, and 19**. This material is available free of charge via the Internet at <http://pubs.acs.org>. JO0499266

(74) Lammertsma, K.; Güner, O. F.; Thibodeaux, A. F.; Schleyer, P. v. R. *J. Am. Chem. Soc.* **1989**, *111*, 8995–9002.

(75) Mayer, P. M.; Radom, L. *Chem. Phys. Lett.* **1997**, *280*, 244–250.

(76) Ault, A.; Kopet, R.; Serianz, A. *J. Chem. Educ.* **1971**, *48*, 410–411.

(77) Schonberg, A.; Soddke, U.; Praefcke, K. *Chem. Ber.* **1969**, *102*, 1453–1467.

(78) Frisch, M. J.; Trucks, G. W.; Schlegel, H. B.; Scuseria, G. E.; Robb, M. A.; Cheeseman, J. R.; Zakrzewski, V. G.; Montgomery, J. A., Jr.; Stratmann, R. E.; Burant, Dapprich, S.; Millam, J. M.; Daniels, A. D.; Kudin, K. N.; Strain, M. C.; Farkas, O.; Tomasi, J.; Barone, V.; Cossi, M.; Cammi, R.; Mennucci, B.; Pomelli, C.; Adamo, C.; Clifford, S.; Ochterski, J.; Petersson, G. A.; Ayala, P. Y.; Cui, Q.; Morokuma, K.; Malick, D. K.; Rabuck, A. D.; Raghavachari, K.; Foresman, J. B.; Cioslowski, J.; Ortiz, J. V.; Baboul, A. G.; Stefanov, B. B.; Liu, G.; Liashenko, A.; Piskorz, P.; Komaromi, I.; Gomperts, R.; Martin, R. L.; Fox, D. J.; Keith, T.; Al-Laham, M. A.; Peng, C. Y.; Nanayakkara, A.; Gonzalez, C.; Challacombe, M.; Gill, P. M. W.; Johnson, B. G.; Chen, W.; Wong, M. W.; Andres, J. L.; Gonzalez, C.; Head-Gordon, M.; Replogle, E. S.; Pople, J. A. *Gaussian 98*, rev. A.7; Gaussian, Inc.: Pittsburgh, PA, 1998.

(79) Frisch, M. J.; Trucks, G. W.; Schlegel, G. W.; Scuseria, G. E.; Robb, M. A.; Cheeseman, J. R.; Montgomery, J. A. J.; Vreven, T.; Kudin, K. N.; Burant, J. C.; Millam, J. M.; Iyengar, S. S.; Tomasi, J.; Barone, V.; Mennucci, B.; Cossi, M.; Scalmani, G.; Rega, N.; Petersson, G. A.; Nakatsuji, H.; Hada, M.; Ehara, M.; Toyota, K.; Fukuda, R.; Hasegawa, J.; Ishida, M.; Nakajima, T.; Honda, Y.; Kitao, O.; Nakai, H.; Klene, M.; Li, X.; Knox, J. E.; Hratchian, H. P.; Cross, J. B.; Adamo, C.; Jaramillo, J. J.; Gomperts, R.; Stratmann, R. E.; Yazyev, O.; Austin, A. J.; Cammi, R.; Pomelli, C.; Ochterski, J. W.; Ayala, P. Y.; Morokuma, K.; Voth, G. A.; Salvador, P.; Dannenberg, J. J.; Zakrzewski, V. G.; Dapprich, S.; Daniels, A. D.; Strain, M. C.; Farkas, O.; Malick, D. K.; Rabuck, A. D.; Raghavachari, K.; Foresman, J. B.; Ortiz, J. V.; Cui, Q.; Baboul, A. G.; Clifford, S.; Cioslowski, J.; Stefanov, B. B.; Liu, G.; Liashenko, A.; Piskorz, P.; Komaromi, I.; Martin, R. L.; Fox, D. J.; Keith, T.; Al-Laham, M. A.; Peng, C. Y.; Nanayakkara, A.; Challacombe, M.; Gill, P. M. W.; Johnson, B. J.; Chen, W.; Wong, M. W.; Gonzalez, C.; Pople, J. A. *Gaussian 03*, rev. B.03; Gaussian, Inc.: Pittsburgh, PA, 2003.